Heliyon 10 (2024) e33494

Contents lists available at ScienceDirect

Heliyon

journal homepage: www.cell.com/heliyon

Research article

Structural changes in amide I and amide II regions of PCOS women analyzed by ATR-FTIR spectroscopy

Mandeep Kaur, Sukhjashanpreet Singh, Anupam Kaur *

Department of Human Genetics, Guru Nanak Dev University, Amritsar, Punjab, 143005, India

ARTICLE INFO

Keywords:
FTIR
PCOS phenotypes
Principal component analysis
Hierarchical cluster analysis

ABSTRACT

The etiology of PCOS is complex and frequently mis or undiagnosed, which may enhance morbidity and reduce the quality of life. Attenuated total reflection- Fourier transform infrared (ATR-FTIR) spectroscopy examines the structural fingerprints of the biochemical compounds and can provide distinct FTIR spectra of the PCOS cases and controls. The present study recruited 61 PCOS cases and 38 control women. The student's t-test was used to compare BMI, WHR, and lipid profile. The FTIR spectral region was compared among both groups using the Mann-Whitney *U* test and multivariate analysis involved principal component analysis (PCA) and hierarchical cluster analysis (HCA). FTIR spectra of different phenotypes of PCOS were also analyzed using multivariate analysis. In univariate analysis, PCOS women had significantly higher WHR ($p = 0.007$), BMI ($p = 0.04$), triglycerides ($p = 0.04$), and VLDL ($p = 0.02$) than the controls. The spectral regions of amide I (1700-1600 cm-1) and amide II (1580-1480 cm-1), were significantly greater in the PCOS group than in the controls ($p < 0.01$ and $p < 0.001$, respectively). The PCA and HCA revealed a distinct molecular fingerprint for phenotype A (PCOM + OA + HA) and phenotype B (HA + OA).

Our study postulated that the spectral regions of amide I and amide II can distinguish between PCOS cases and control women and it may be used for the diagnosis of cases.

Ethics approval

The study was approved by the Ethical Committee of Guru Nanak Dev University (No.296/HG) on 07-04-2022, consistent with provisions of the Declaration of Helsinki.

Consent to participate

The informed consent was taken from all the study participants.

1. Introduction

Polycystic ovary syndrome (PCOS) is one of the most prevalent endocrine disorders among females of reproductive age,

* Corresponding author.
E-mail addresses: mandeepkaur.mk1995@gmail.com, mandeephuman.rsh@gndu.ac.in (M. Kaur), jashanbal5@gmail.com, sukhjashanhuman.rsh@gndu.ac.in (S. Singh), anupamkaur@yahoo.com, anupam.human@gndu.ac.in (A. Kaur).

https://doi.org/10.1016/j.heliyon.2024.e33494
Received 16 February 2024; Received in revised form 20 June 2024; Accepted 21 June 2024
Available online 26 June 2024

characterized by irregular periods, hyperandrogenism, and polycystic ovaries. The clinical manifestations of PCOS include hirsutism, irregular menstruation, chronic anovulation, cystic acne, alopecia, and infertility [1]. As one of the leading causes of female infertility, prevalence is claimed to be 6–26 % worldwide [2–4]. Women with PCOS exhibit a greater susceptibility to experiencing T2DM, infertility, obstetrical difficulties, endometrial cancer, and mood disorders. Besides, these women are also more likely to suffer cardiovascular and cerebrovascular problems, venous thromboembolism, and ovarian cancer [5].

PCOS is often diagnosed using the Rotterdam criteria, which require the presence of two out of three features: chronic anovulation, clinical or biochemical hyperandrogenism, or polycystic ovary morphology (PCOM) [6]. During adolescence, gonadotropin secretion increases, resulting in larger ovaries and symptoms of excessive androgen levels, such as cystic acne. These symptoms can sometimes make it challenging to diagnose PCOS because they overlap with normal physiology during adolescence. Furthermore, the assessment of biochemical hyperandrogenism entails expensive tests such as testosterone and DHEAS, which have limited sensitivity [1]. Misdiagnosis or improper diagnosis of PCOS can lead to inappropriate management. This condition impacts the biochemical pathway responsible for carbohydrates, lipids, nucleic acid, and protein metabolism, resulting in widespread effects throughout the body. Unfortunately, no established method can comprehensively understand the differences in the molecular makeup of PCOS and healthy women. It would be intriguing to employ spectroscopic techniques alongside the standard method to compare and enhance therapeutic management [7].

Attenuated total reflection-fourier transform infrared (ATR-FTIR) spectroscopy is an excellent analytical technique for understanding the molecular composition of body fluids such as blood serum, plasma, tears, urine, and others [8,9]. This technique helps to provide biochemical fingerprints of cellular macromolecules such as lipids, proteins, carbohydrates, nucleic acids, and phosphorylated compounds, at different spectral regions [10]. Due to its efficiency, cost-effectiveness, less time consuming, and reagent-free sample preparation, it is a potent method to be utilized extensively across various sectors for exploring cells and other biomedical materials.

Only a few studies conducted worldwide have explored the potential of ATR-FTIR to gain insights into functional biochemical signatures in PCOS cases. Guleken et al. conducted a study in 2020 and found a notable distinction in the functional spectra between early-age PCOS girls and non-adolescent PCOS women [8]. Salman et al. [11] also found a positive correlation between the spectral region of the protein's secondary structure and PCOS. However, they did not conduct a study to analyze the biochemical signatures among the different phenotypes of PCOS. Thus, our study focused on utilizing FTIR spectroscopy to identify the specific spectral region that can differentiate between women with PCOS and those who are healthy. In addition, we wanted to examine whether the PCOS phenotypes had different FTIR spectra.

2. Material and methodology

2.1. Sample collection

The Institutional Ethics Committee (IEC) at Guru Nanak Dev University, Amritsar, Punjab, approved the current study. The study consisted of a total of 99 subjects, 61 women with PCOS and 38 age-matched healthy women (without any sign of metabolic and reproductive disorders) and these were the archived samples [12]. The Rotterdam criterion was used to diagnose PCOS and this study excluded subjects exhibiting signs of Cushing syndrome, congenital hyperplasia, androgen-secreting tumors, and thyroid dysfunction.

2.2. Biochemical analysis

Lipid profiles including cholesterol, triglycerides, and high-density lipoprotein (HDL) levels were measured and methods were explained in our previous study [4]. Low-density lipoprotein (LDL) and very low-density lipoprotein (VLDL) levels were calculated using Friedwald's formula [13].

2.3. Different phenotypes of PCOS

PCOS cases are divided into 4 phenotypes based on their characteristic features. PCOS phenotypes include phenotype-A (hyperandrogenism + oligomenorrhea + polycystic ovarian morphology), phenotype-B (hyperandrogenism + oligomenorrhea), phenotype-C (hyperandrogenism + polycystic ovarian morphology), and phenotype-D (oligomenorrhea + polycystic ovarian morphology) [14].

2.4. FTIR spectroscopy

An experiment was performed with a Cary 630 FTIR spectrometer in the 4000 to 400 cm−1 range. An FTIR imaging system was programmed for 64 scans at 16 cm−1 resolution, and the measurements took 30 s. For FTIR, 30 μl of the serum samples were freeze-dried using a vacuum concentrator. The diamond ATR sensor was cleaned with HPLC-grade ethyl alcohol, and the initial diamond ATR unit was recorded as blank and subtracted to remove the effects of surrounding air, before each sample measurement. All spectral pre-processing was performed using Agilent Micro Lab Expert software. Baseline correction using the rubber band method [15] and 16 points smoothened (Polynomial 4) with Savitzky–Golay from 4000 to 600 cm−1 bands were performed to eliminate sharp bands in the spectral region [16] and then averaged, and a second derivative was calculated [17,18].

2.5. Statistics

In univariate statistical analysis, student's t-test (GraphPad Prism 9 - Graph Pad Software, Inc.) for lipid profile and other characteristic features. To calculate the peak area for FTIR spectra Mann-Whitney *U* test was performed. The statistical significance was considered if the p-value was less than or equal to 0.05.

In multivariate analysis, Principal component analysis (PCA) and Hierarchical cluster analysis (HCA) were used to gather data regarding the spectra variance among the samples. PCA minimized the number of variables, or dimensions, in the data while preserving as much variance as possible. Consequently, HCA offers a comprehensible method for examining interrelationships among clusters that cannot be achieved using non-nested techniques. Using Origin Pro software, PCA and HCA were conducted in the region corresponding to functional groups (1400-1100cm-1 and 1700-1400cm-1) to investigate the distinguishable features of FTIR spectra among cases and controls along with various PCOS phenotypes.

3. Results

3.1. Characteristic features

A total of 99 women were recruited out of which 61 were PCOS cases and 38 were healthy controls. The average age of PCOS women is 22.54 ± 2.3 and of controls 23.34 ± 3.4. The obesity-related parameters such as BMI and WHR are significantly higher in PCOS cases than in the control group (BMI: 23.9 ± 3.5; 22.4 ± 1.1, $p = 0.04$; WHR: 0.85 ± 0.06; 0.81 ± 0.06, $p = 0.007$, respectively). Lipid profile was also compared between both the groups and triglycerides and VLDL levels were higher in cases than in the control group with p-values 0.04 and 0.02 respectively (Table 1).

3.2. FTIR spectroscopy analysis

The FTIR spectra of cases and controls were compared to examine the biomolecular changes due to PCOS. The averaged spectra (without second derivative) of PCOS cases and controls were shown in Fig. 1, due to lower resolution, the second derivative was calculated from spectral data [19]. A specific IR range for biological material corresponds to the functional groups that make the structures of nucleic acids, carbohydrates, proteins, and fatty acids. Table 2 shows the different spectral ranges with their specific biomolecule assignment. Most information on the proteins including amide I and amide II and secondary structure is found in the range 1700–1400 cm-1. The oscillations of functional groups such as PO_2, C–O, and C–C, found in proteins, lipids, nucleic acids, and carbohydrates are present in a range of 1400–1000 cm-1 [20–25]. A significant difference ($p < 0.05$) was found within the spectral range (1700-1600cm-1 and 1580-1480cm-1) among PCOS cases and controls (Fig. 2). This difference in IR spectra might be due to the structural and quantitative changes.

1. Amide I and Amide II region analysis:

The second derivative FTIR spectra (1700- 1400 cm-1) of serum samples of PCOS women and controls are shown in Fig. 3. A difference in the absorbance was found in the 1700-1600 cm-1 which generally corresponds to amide I and can be used to investigate the secondary structure of a globular protein [20]. A region of 1699 to 1662 cm-1 corresponds to antiparallel beta sheets and in this region decreased absorbance at 1699 cm-1 was observed. Further absorbance difference was noted at 1662 cm-1 and 1669 cm-1. Alpha-helix structures were recorded near (1654 cm-1). Likewise, IR spectra of 1630–1637 cm-1 and 1611-1630 cm-1, known as beta-sheet and cross beta-sheet region, had higher absorbance in PCOS than control women. Spectral region∼ 1580-1480 cm-1 corresponds to the amide II region [26] and showed higher absorption in PCOS cases specifically at 1505 cm-1 and 1528 cm-.

2. Nucleic acid and Carbohydrate analysis:

Table 1
Characteristic features of PCOS cases and Controls.

	PCOS Cases (61)	Controls (38)	p-value
Age	22.54 ± 2.3	23.34 ± 3.4	0.6
BMI	23.9 ± 3.5	22.4 ± 1.1	**0.04**[a]
WHR	0.85 ± 0.06	0.81 ± 0.06	**0.007**[a]
Cholesterol	170.64 ± 44.1	166.4 ± 44.1	0.5
Triglycerides	134.31 ± 81	101.25 ± 42.5	**0.04**[a]
HDL-C	43.24 ± 16.1	47.3 ± 16.6	0.2
LDL-C	99.26 ± 34.9	109.08 ± 52.2	0.3
VLDL-C	27.4 ± 16.1	20.25 ± 8.51	**0.02**[a]

BMI- Body mass index, WHR- Waist Hip Ratio, HDL, High-Density Lipoprotein, LDL-Low density lipoprotein, VLDL-Very low-density lipoprotein.

[a] p-value considered significant at <0.05.

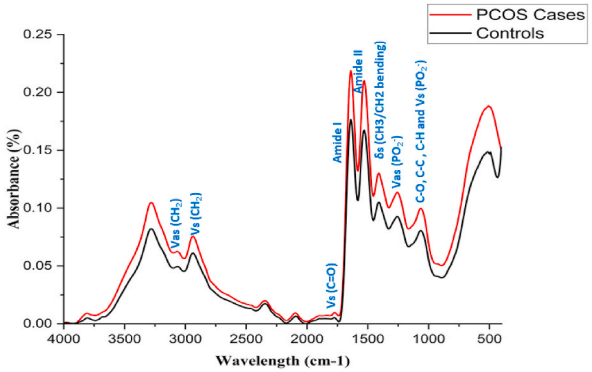

Fig. 1. Averaged FTIR spectra for PCOS cases (Black) and controls (red).

Table 2
Distinguished infrared spectral bands with biomolecular assignments, Adapted from Refs. [20,22–25,36].

Sr. No.	Wavenumber region (cm-1)	Biomolecule Assignment
1.	1000–1140	Carbohydrates and nucleic acids: C–O, C–C stretch, C–H bend, deoxyribose/ribose DNA, RNA, *νs* (PO2 −).
2.	1190–1240	Asymmetric phosphate I: *νas* (PO2 −) of lipid phosphates.
3.	1250–1350	Amide III of proteins (CH3 and C–C stretching vibrations)
4.	1325–1380	C–H deformation: due to CH3/CH2 bending (groups in α and β anomers) of lipids and proteins.
5.	1480–1580	Amide II of proteins: (α-helical, β-pleated sheet, unordered conformation structures), δ(N–H), *ν*(C–N)
6.	1600–1700	Amide I of proteins: (α-helical, β-pleated sheet, β-turns, cross beta-sheet, and side-chain structures), *ν*(C═O), *ν*(C–N), CNN.

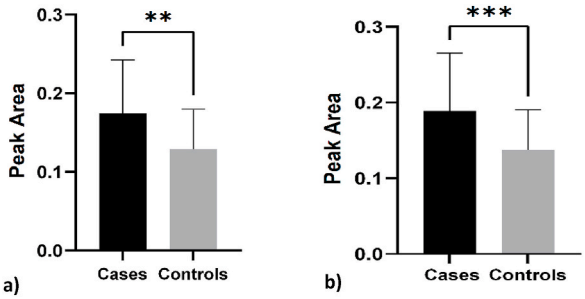

Fig. 2. FTIR Spectral area among both the groups: a) Amide I region (1700-1600cm-1) b) Amide II region (1580-1480 cm-1) (Mann-Whitney *U* test was applied; ** and *** -p-value considered significant at <0.01 and < 0.001 p-value).

Fig. 4 illustrates multiple overlapping vibrations predominantly of nucleic acid and carbohydrates in the spectral range of 1140–1000 cm-1 [27,28]. In PCOS women, a wave shift and absorption difference were seen at the 1118-1110 cm-1 region, which is primarily associated with RNA absorbance, while for DNA absorbance which is noted near 1021cm-1 [29], no structural and quantitation difference was found among both the groups. Region 1140 cm-1 corresponds to the stretching at the C–OH bond in the membrane-bound oligosaccharides [27]. While regions near 1030cm-1 and 1076 cm-1 are due to the presence of anomers of glucose and mannose respectively [20]. Asymmetric and symmetric stretching in the PO_2^- the group was located on 1185 cm-1 and 1080 cm-1 respectively [30]. Absorbance difference was seen in methyl-related (-CH3) and C–C stretching vibrations of amide III, positioned on 1350-1250cm-1 as multiple peaks [31], in addition, morphological change was also detected near 1319 cm-1.

3. PCA and HCA analysis

Principal component analysis (PCA) was performed on the FTIR spectra to ascertain which FTIR region might be useful in differentiating controls from PCOS women. PCA analysis was done on spectral regions where functional groups of biomolecules are present, which includes regions 1400 to 1000 cm-1 and 1700 to 1400 cm-1 shown in Figs. 5 and 6 respectively. The contribution of principal component 2 (PC2) is less than 2 %, which does not significantly impact clustering. From the PCA of region 1400 to 1000 cm-1 and 1700 to 1400 cm-1, it was found that controls were majorly placed in the negative area of PC1, and a cluster of PCOS women is located in the positive and negative area of PC1. Also, the 95 % confidence eclipse, which corresponds to variance, is smaller for

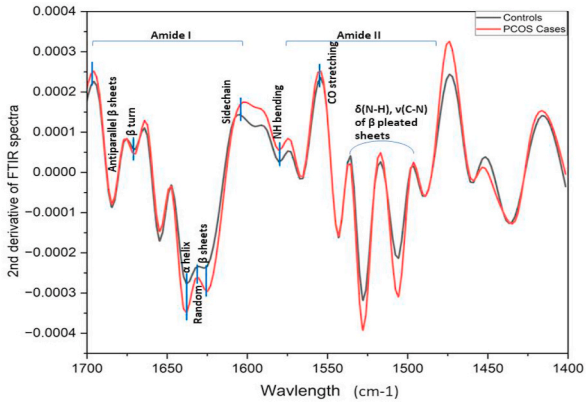

Fig. 3. Representation of the second derivative of IR spectral region 1700-1400 cm-1 demonstrating differences between PCOS cases (red) and controls (black) in the Amide I and Amide II regions.

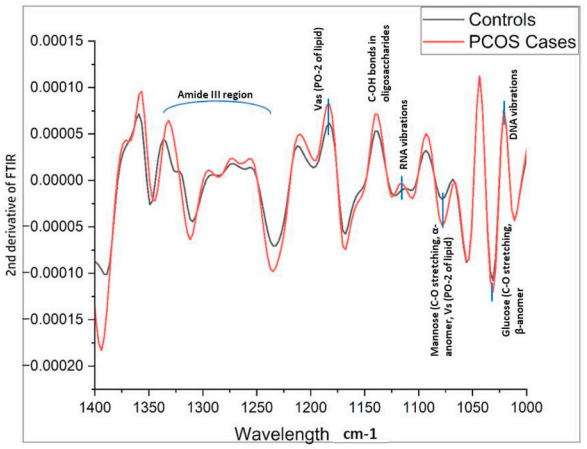

Fig. 4. FTIR spectral region 1400-1000 cm-1 demonstrating differences between PCOS cases (red) and controls (black).

controls than the eclipse of PCOS women. The score plots revealed that clusters are not distinctly separated while some PCOS cases are located differently from controls (Figs. 5 and 6).

Hierarchical clustering analysis is frequently utilized to ascertain similarities among FTIR spectra. This is achieved by calculating the distances between spectra by Ward's algorithm and squared Euclidean distance measurements. Results were analyzed while performing the HCA, at 50 % cut-off and it was found that out of the four clades, one clade contained only PCOS cases, and other clades had both PCOS cases and healthy women for spectral regions 1400 to 1000 cm-1 and 1700 to 1400 cm-1 as shown in Fig. 7 (a and b).

We further stratified PCOS cases according to the different Rotterdam phenotypes: Phenotypes A, B, C, and D, Both PCA and HCA analyses were performed to analyze any metabolic changes within PCOS phenotypes. It was noted that PCOS women with classic phenotype (Phenotype A) were clustered in the positive of PC1 and were differentiated from the other phenotypes. The FTIR spectra of phenotype C and D were similar as both grouped in negative and positive of PC1, while PCOS women belonging to phenotype B were also clustered separately from the other phenotypes (Fig. 8a).

The dendrogram for HCA was generated using ATR-FTIR spectra of different PCOS phenotypes A, B, C, and D, as depicted in Fig. 8b which facilitates the identification of sub-groups within the dataset. The A phenotype spectra have a particular clustering pattern, wherein they are clustered together based on a high level of similarity within each group or clustered with phenotype B. Likewise, a notable clustering pattern is observed in the phenotypes B, C and D, indicating greater heterogeneity within the spectra of these 3 groups. At a similarity threshold of 50 %, our analysis revealed the presence of four primary clades. Within two of these clades, A and B phenotypic spectra were observed. Another clade consisted only of phenotypes C and D, while the remaining clade encompassed all four phenotypic spectra (Fig. 8b).

4. Discussion

Vibrational spectroscopy analysis in serum and other biological fluids has been thoroughly studied. This is because it is easily

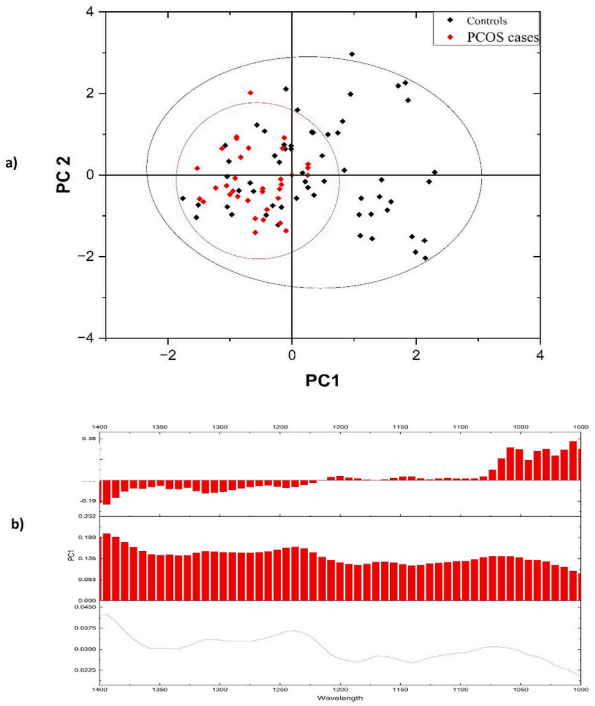

Fig. 5. a) PCA analysis of PCOS cases (red dot) and Controls (black dot) samples from ranges (1400–1000 cm-1), b) representation of loadings of PC1 and PC2 with reference for FTIR spectra (1400–1000 cm-1).

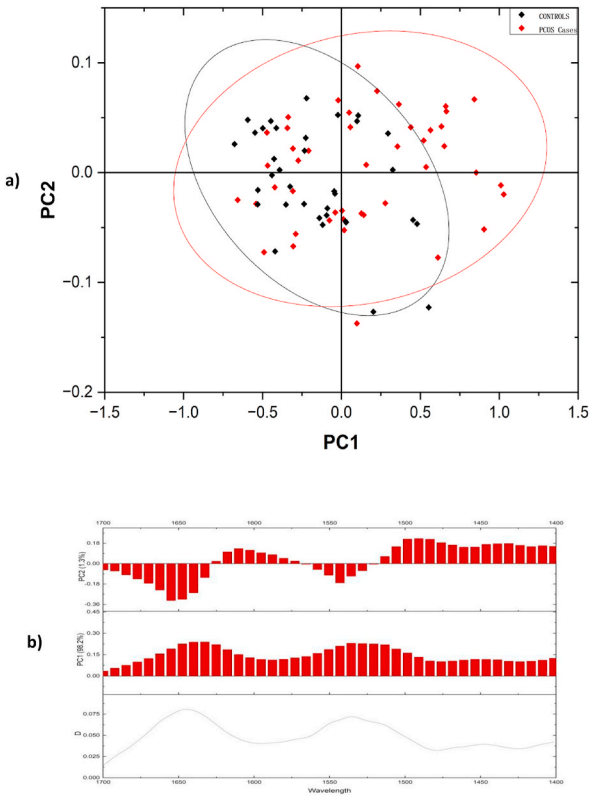

Fig. 6. a) PCA analysis of PCOS cases (red dot) and Controls (black dot) samples from ranges (1700–1400 cm-1), b) representation of loadings of PC1 and PC2 with reference for FTIR spectra (1700–1400 cm-1).

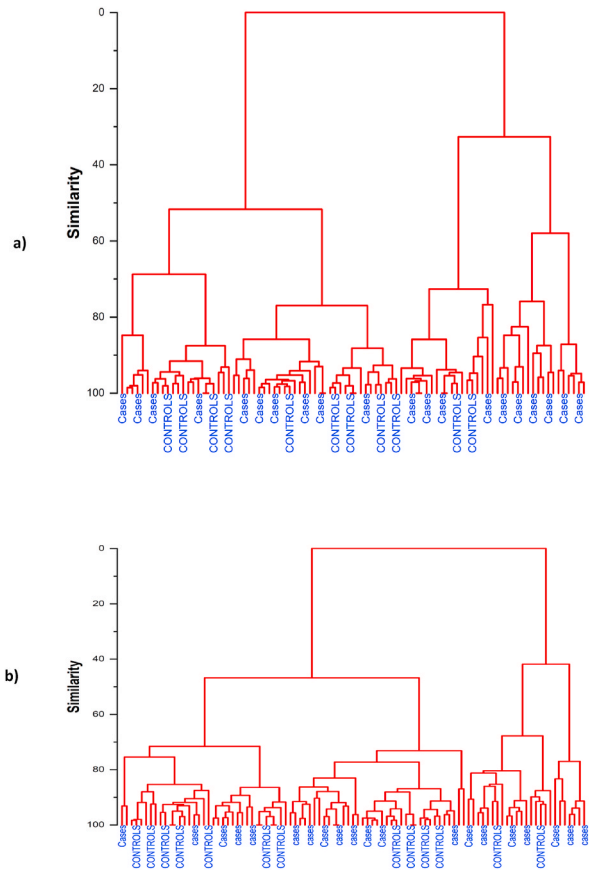

Fig. 7. Hierarchical clustering analysis of FTIR spectral region a) 1400-1000 cm-1, b)1700 -1400 cm-1.

accessible and provides valuable information about the molecular composition of these fluids, which can indicate different patho-physiological conditions. The FTIR-ATR technique is widely regarded as a highly effective method for analyzing the molecular composition of biofluids in both normal and pathological [32,33]. The utilization of FTIR-ATR spectroscopy has emerged as a valuable diagnostic tool for various diseases, including ovarian and breast cancer, Alzheimer's disease, and brain tumors [24,34,35].

In the present study, we investigated the FTIR spectra of 61 PCOS women and 38 healthy women along with lipid profiles. Our results showed a significant difference in triglyceride and VLDL levels among both groups. From the FTIR spectra, higher levels of protein components were observed in the PCOS women than in the controls (Fig. 2).

FTIR spectra have been divided into their different spectral bands, which contain most of the functional groups of biomolecules. These ranges are 1000–1400cm-1 and 1700-1400 cm-1, first containing information about the functional group of lipid, amide III, nucleic acid and carbohydrates, and the subsequent spectral range corresponds to amide I and amide II bands of proteins. In both spectral ranges, a slight morphological change was observed at the RNA region (near 1118-1110 cm-1) and in the region of the amide III band. Moreover, the amide I (1700-1600 cm-1) and amide II (1580-1480 cm-1) regions which are assumed to be important regions for the characterization of protein, indicate significant structural differences in both groups (Fig. 2). It may be noted that amide III is also an important region to examine the secondary structure in proteins [36]. When multivariate analysis (PCA and HCA) was applied to FTIR spectra of serum samples of PCOS cases and the control group, it was observed that the samples did not exhibit clear clustering into two distinct groups. Similarly, Salman et al. [11] did an FTIR spectral analysis in PCOS women and did not find any separate clusters of PCOS women and controls in PCA analysis. They also found significant differences in the amide I and amide II spectral regions, that support our study. While, they also observed that the lipid spectral region, at 2846, 2848, 2850, 2852, 2854, and 2916 cm-1 had more absorption with PCOS however, no significant difference of this spectral region was seen in our study. In contrast to the present study, Guleken and colleagues conducted FTIR spectral analysis and showed distinct clusters among PCOS cases and controls for nucleic acid, lipids, and proteins. Moreover, they divided PCOS women into two groups: those above 25 age and under 25 ages and found that the spectral signatures of those under 25 PCOS women were the same as the controls [8].

Similarly, Salman et al. [11] conducted an FTIR spectral analysis on PCOS women and found no separate clusters of PCOS women and controls in the PCA analysis. They also found significant changes in the amide I and amide II spectral regions, thus, supporting our study. However, they also noted that PCOS increased absorption in the lipid spectral region at 2846, 2848, 2850, 2852, 2854, and 2916 cm-1 while our study did not find significant differences in these spectral regions. Guleken and colleagues conducted FTIR spectral analysis on the serum samples of PCOS cases and controls. They demonstrated a visible separation of clusters of PCOS and healthy

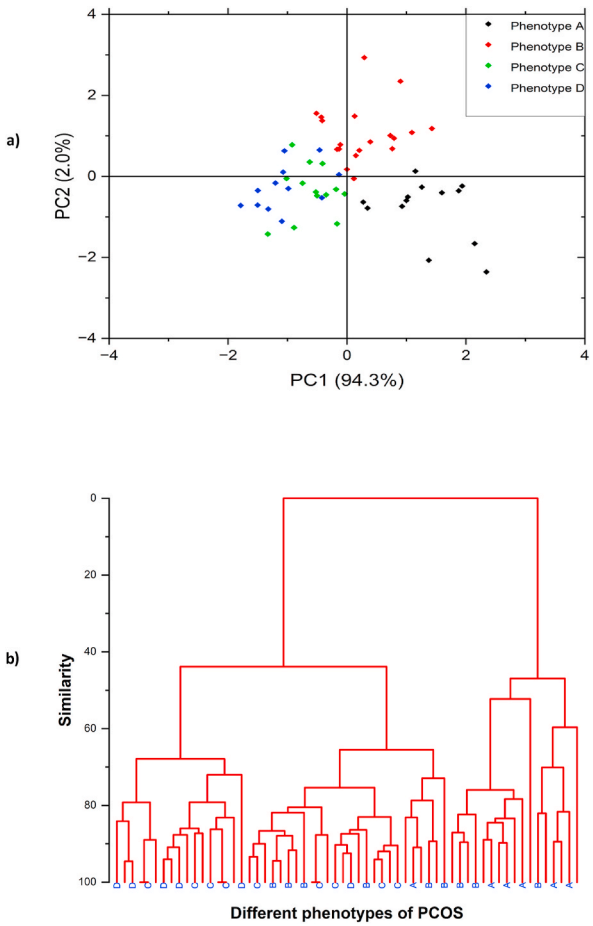

Fig. 8. a) PCA analysis b) HCA analysis of FTIR spectra of different phenotypes of PCOS.

women for the nucleic acid, lipids, and proteins, which contradicts our findings. Moreover, they divided PCOS women into two groups: those above 25 age and under 25 age and found that the spectral signatures of those under 25 PCOS women were the same as those of controls [8].

We also found that the FTIR spectra of PCOS phenotypes C and D exhibit greater similarities than phenotypes A and B (Fig. 8a). PCOS women with phenotypes A and B exhibited distinct FTIR spectra indicating the presence of unique patterns of metabolites compared to those with other phenotypes. Phenotype A showed a higher occurrence of obesity, hyperandrogenism, insulin resistance, abnormal lipid profile, and metabolic syndrome when compared with other phenotypes [37]. Thus, there is a higher probability of experiencing negative metabolic and cardiovascular outcomes with phenotype A.

5. Conclusion

This study aimed to determine whether FTIR spectroscopy can distinguish between PCOS and healthy women. The study concluded that the peak area of amide I and amide II spectral regions (IR1450 to 1700 cm-1) is significantly higher in the PCOS. The FTIR spectra of PCOS women having phenotypes A and B were distinct from C and D phenotypes, as demonstrated by PCA and HCA analysis. This finding provides insight into the unique metabolic patterns present among various phenotypes. This is the first study of its kind to be conducted in India that utilized ATR-FTIR spectroscopy to differentiate the serum samples of PCOS cases and controls. Additionally, to the best of our knowledge, we are the first group that used ATR-FTIR spectroscopy to analyze the difference between the biochemical signatures in serum samples across different PCOS phenotypes. We recommended conducting FTIR spectroscopy on a large sample size to gain further insight into the structural changes in PCOS phenotypes. FTIR spectroscopy offers a compelling alternative for PCOS diagnosis due to its several advantages. Minimal sample preparation makes it a time-efficient and cost-effective method compared to traditional methods. Additionally, it requires just 30 μl of sample to obtain complete molecular spectra with higher sensitivity, which reduces patient discomfort. Unlike current diagnostic methods that require specific timing within the menstrual cycle and potentially multiple visits, FT-IR could offer greater flexibility to patients. Understanding FT-IR spectroscopy can be challenging for beginners because of its complicated statistical approach to analyzing spectra. However, we believe the widespread adoption of this technique and the simplified statistical approach can inspire clinicians to familiarize themselves with FT-IR and its potential for diagnosing,

monitoring, and evaluating diseases.

Data availability statement

- Research-related data is not deposited in publicly available repositories
- The data given in the manuscript will be available on request.

CRediT authorship contribution statement

Mandeep Kaur: Writing – review & editing, Writing – original draft, Methodology, Investigation, Formal analysis. **Sukhjashanpreet Singh:** Methodology, Investigation. **Anupam Kaur:** Visualization, Supervision, Conceptualization.

Declaration of competing interest

The authors declare that they have no known competing financial interests or personal relationships that could have appeared to influence the work reported in this paper.

Acknowledgment

The authors are thankful to Dr. Ritu Bala (Assistant Professor, Chemistry Department at Guru Nanak Dev University) for the ATR-FTIR facilitation. MK and SS sincerely acknowledge the financial support provided by the University Grants Commission - Senior Research Fellowship (UGC-SRF).

References

[1] S.F. Witchel, S.E. Oberfield, A.S. Peña, Polycystic ovary syndrome: pathophysiology, presentation, and treatment with emphasis on adolescent girls, J. Endocr. Soc. 3 (2019) 1545–1573.
[2] X. Chen, D. Yang, Y. Mo, L. Li, Y. Chen, Y. Huang, Prevalence of polycystic ovary syndrome in unselected women from southern China, Eur. J. Obstet. Gynecol. Reprod. Biol. 139 (2008) 59–64.
[3] M.P. Lauritsen, J.G. Bentzen, A. Pinborg, A. Loft, J.L. Forman, L.L. Thuesen, A. Cohen, D.M. Hougaard, A. Nyboe Andersen, The prevalence of polycystic ovary syndrome in a normal population according to the Rotterdam criteria versus revised criteria including anti-Müllerian hormone, Hum. Reprod. 29 (2014) 791–801.
[4] S. Singh, M. Kaur, R. Kaur, A. Beri, A. Kaur, Association analysis of LHCGR variants and polycystic ovary syndrome in Punjab: a case–control approach, BMC Endocr. Disord. 22 (2022) 335.
[5] R. Azziz, E. Carmina, Z. Chen, A. Dunaif, J.S. Laven, R.S. Legro, D. Lizneva, B. Natterson-Horowtiz, H.J. Teede, B.O. Yildiz, Polycystic ovary syndrome, Nat. Rev. Dis. Prim. 2 (2016) 1–18.
[6] A.H. Balen, Polycystic ovary syndrome (PCOS), Obstet. Gynecol. 19 (2017) 119–129.
[7] N.M. de Souza, B.H. Machado, A. Koche, L.B. da Silva Furtado, D. Becker, V.A. Corbellini, A. Rieger, Detection of metabolic syndrome with ATR-FTIR spectroscopy and chemometrics in blood plasma, Spectrochim. Acta, Part A 5 (288) (2023) 122135.
[8] Z. Guleken, H. Bulut, B. Bulut, J. Depciuch, Assessment of the effect of endocrine abnormalities on biomacromolecules and lipids by FT-IR and biochemical assays as biomarker of metabolites in early Polycystic ovary syndrome women, J. Pharm. Biomed. Anal. 10 (204) (2021) 114250.
[9] G. Clemens, J.R. Hands, K.M. Dorling, M.J. Baker, Vibrational spectroscopic methods for cytology and cellular research, Analyst 139 (2014) 4411–4444.
[10] G. Güler, U. Guven, G. Oktem, Characterization of CD133+/CD44+ human prostate cancer stem cells with ATR-FTIR spectroscopy, Analyst 144 (2019) 2138–2149.
[11] A.M. Hassan Salman, M.A. Al-Zubaidi, Using fourier transform infrared (FTIR) spectroscopy coupled with multivariate analysis to diagnose polycystic ovary syndrome (PCOS), Sys. Rev. Pharm. 11 (2020) 552–560.
[12] M. Kaur, S. Singh, R. Kaur, A. Beri, A. Kaur, Analyzing the impact of FSHR variants on polycystic ovary syndrome—a case-control study in Punjab, Reprod. Sci. 30 (2023) 2563–2572.
[13] W.T. Friedewald, R.I. Levy, D.S. Fredrickson, Estimation of the concentration of low-density lipoprotein cholesterol in plasma, without use of the preparative ultracentrifuge, Clin. Chem. 18 (1972) 499–502.
[14] S. Mumusoglu, B.O. Yildiz, Polycystic ovary syndrome phenotypes and prevalence: differential impact of diagnostic criteria and clinical versus unselected population, Curr. Opin. Endocr. Metab. Res. 12 (2020) 66–71.
[15] K.R. Bambery, B.R. Wood, D. McNaughton, Resonant Mie scattering (RMieS) correction applied to FTIR images of biological tissue samples, Analyst 137 (2012) 126–132 [CrossRef].
[16] Z. Guleken, H. Bulut, G.İ. Gültekin, S. Arıkan, İ. Yaylım, M.T. Hakan, D. Sönmez, N. Tarhan, J. Depciuch, Assessment of structural protein expression by FTIR and biochemical assays as biomarkers of metabolites response in gastric and colon cancer, Talanta 15 (231) (2021) 122353.
[17] J. Steinier, Y. Termonia, J. Deltour, Comments on smoothing and differentiation of data by simplified least square procedure, Anal. Chem. 44 (1972) 1906–1909.
[18] M.J. Baker, J. Trevisan, P. Bassan, R. Bhargava, H.J. Butler, K.M. Dorling, P.R. Fielden, S.W. Fogarty, N.J. Fullwood, K.A. Heys, C. Hughes, Using Fourier transform IR spectroscopy to analyze biological materials, Nat. Protoc. 9 (2014) 1771–1791.
[19] M. Palencia, Functional transformation of Fourier-transform mid-infrared spectrum for improving spectral specificity by simple algorithm based on wavelet-like functions, J. Adv. Res. 1 (2018) 53–62.
[20] H. Ghimire, M. Venkataramani, Z. Bian, Y. Liu, A.U. Perera, ATR-FTIR spectral discrimination between normal and tumorous mouse models of lymphoma and melanoma from serum samples, Sci. Rep. 7 (2017) 16993.
[21] M.J. Baker, S.R. Hussain, L. Lovergne, V. Untereiner, C. Hughes, R.A. Lukaszewski, G. Thiéfin, G.D. Sockalingum, Developing and understanding biofluid vibrational spectroscopy: a critical review, Chem. Soc. Rev. 45 (2016) 1803–1818.
[22] M. Meurens, J. Wallon, J. Tong, H. Noel, J. Haot, Breast cancer detection by Fourier transform infrared spectrometry, Vib. Spectrosc. 10 (1996) 341–346.
[23] E. Gazi, J. Dwyer, P. Gardner, A. Ghanbari-Siahkali, A.P. Wade, J. Miyan, N.P. Lockyer, J.C. Vickerman, N.W. Clarke, J.H. Shanks, L.J. Scott, Applications of Fourier transform infrared microspectroscopy in studies of benign prostate and prostate cancer. A pilot study, J. Pathol. 201 (2003) 99–108.
[24] J.R. Hands, G. Clemens, R. Stables, K. Ashton, A. Brodbelt, C. Davis, T.P. Dawson, M.D. Jenkinson, R.W. Lea, C. Walker, M.L. Baker, Brain tumour differentiation: rapid stratified serum diagnostics via attenuated total reflection Fourier-transform infrared spectroscopy, J. Neuro Oncol. 127 (2016) 463–472.

[25] K. Gajjar, L.D. Heppenstall, W. Pang, K.M. Ashton, J. Trevisan, I.I. Patel, V. Llabjani, H.F. Stringfellow, P.L. Martin-Hirsch, T. Dawson, F.L. Martin, Diagnostic segregation of human brain tumours using Fourier-transform infrared and/or Raman spectroscopy coupled with discriminant analysis, Anal. Methods 5 (2013) 89–102.
[26] D.M. Byler, H. Susi, Examination of the secondary structure of proteins by deconvolved FTIR spectra, Biopolymers 25 (1986) 469–487.
[27] Z. Movasaghi, S. Rehman, D.I. ur Rehman, Fourier transform infrared (FTIR) spectroscopy of biological tissues, Appl. Spectrosc. Rev. 43 (2008) 134–179.
[28] B.R. Wood, L. Chiriboga, H. Yee, M.A. Quinn, D. McNaughton, M. Diem, Fourier transform infrared (FTIR) spectral mapping of the cervical transformation zone, and dysplastic squamous epithelium, Gynecol. Oncol. 93 (2004) 59–68.
[29] P.G. Andrus, R.D. Strickland, Cancer grading by Fourier transform infrared spectroscopy, Biospectroscopy 4 (1998) 37–46.
[30] C. Petibois, G. Déléris, Oxidative stress effects on erythrocytes determined by FT-IR spectrometry, Analyst 129 (2004) 912–916.
[31] Y. Ji, X. Yang, Z. Ji, L. Zhu, N. Ma, D. Chen, X. Jia, J. Tang, Y. Cao, DFT-calculated IR spectrum amide I, II, and III band contributions of N-methylacetamide fine components, ACS Omega 5 (2020) 8572–8578.
[32] B.G. Kim, E.M. Jo, G.Y. Kim, D.S. Kim, Y.M. Kim, R.B. Kim, B.S. Suh, Y.S. Hong, Analysis of methylmercury concentration in the blood of Koreans by using cold vapor atomic fluorescence spectrophotometry, Ann. Lab. Med. 32 (2012) 31–37.
[33] P. Guang, W. Huang, L. Guo, X. Yang, F. Huang, M. Yang, W. Wen, L. Li, Blood-based FTIR-ATR spectroscopy coupled with extreme gradient boosting for the diagnosis of type 2 diabetes: a STARD compliant diagnosis research, Medicine 99 (2020) e19657.
[34] M. Paraskevaidi, C.L. Morais, K.M. Lima, J.S. Snowden, J.A. Saxon, A.M. Richardson, M. Jones, D.M. Mann, D. Allsop, P.L. Martin-Hirsch, F.L. Martin, Differential diagnosis of Alzheimer's disease using spectrochemical analysis of blood, Proc. Nation. Acad. Sci. 114 (2017) E7929–E7938.
[35] K.M. Lima, K.B. Gajjar, P.L. Martin-Hirsch, F.L. Martin, Segregation of ovarian cancer stage exploiting spectral biomarkers derived from blood plasma or serum analysis: ATR-FTIR spectroscopy coupled with variable selection methods, Biotechnol. Prog. 31 (2015) 832–839.
[36] B.R. Singh, D.B. DeOliveira, F.N. Fu, M.P. Fuller, Fourier transform infrared analysis of amide III bands of proteins for the secondary structure estimation, Biomolecular spectroscopy III 1890 (1993) 47–55.
[37] G. Sachdeva, S. Gainder, V. Suri, N. Sachdeva, S. Chopra, Comparison of the different PCOS phenotypes based on clinical metabolic, and hormonal profile, and their response to clomiphene, Indian J. Endocrinol. Metab 23 (2019) 326–331.